PHYSICAL REVIEW E **77**, 055307(R) (2008)

Highly nonlinear Bragg quasisolitons in the dynamics of water waves

V. P. Ruban*
Landau Institute for Theoretical Physics, 2 Kosygin Street, 119334 Moscow, Russia
(Received 28 March 2008; published 29 May 2008)

Finite-amplitude gravity water waves in Bragg resonance with a periodic one-dimensional topography are studied numerically using exact equations of motion for ideal potential free-surface flows. Spontaneous formation of highly nonlinear localized structures is observed in the numerical experiments. These coherent structures consisting of several nearly standing extreme waves are similar in many aspects to the Bragg solitons previously known in nonlinear optics.

DOI: 10.1103/PhysRevE.77.055307 PACS number(s): 47.15.K−, 47.35.Bb, 47.35.Lf, 47.11.−j

The problem of water wave propagation over a nonuniform bed has been studied for many years mainly in low-amplitude and/or weakly dispersive regimes, or for a mild-slope bottom (see Refs. [1–12], and references therein). For instance, the linear theory has produced many interesting results. In particular, if the bottom topography is periodic, then an important phenomenon takes place, the Bragg reflection of waves which satisfy the resonance conditions $n\lambda=2\Lambda$, where Λ is a spatial period of the bed structure, λ is the wave length, and $n=1,2\ldots$ is an integer number. However, the case of high-amplitude water waves in the Bragg resonance with a periodic bed was not investigated. In the present paper, the interaction of fully nonlinear planar waves with a strongly undulating, nearly periodic one-dimensional (1D) topography is considered. As we know from nonlinear optics, periodic nonlinear media can support very interesting localized waves as Bragg solitons (alternatively called gap solitons; see, e.g., Refs. [13–22]). Also in the field of Bose-Einstein condensation, Bragg solitons have been studied [23–25]. As to the free-surface hydrodynamics, analogous nonlinear structures have not been described up to now. Therefore the main goal of the present work has been to examine if analogous Bragg solitons are possible in water-wave systems. For this purpose, exact evolutionary equations for potential water waves over an arbitrary nonuniform 1D bed, derived by the present author in Ref. [26], were solved numerically. A few tens of numerical experiments have been carried out, for slightly different bottom configurations. An initial state in each case was a moderate-amplitude standing wave (either slowly modulated or not) satisfying the main Bragg resonance condition $\lambda=2\Lambda$. It should be noted, there are two kinds of such standing waves: cos-type waves, with maxima and minima of the free surface elevation (and of the surface velocity potential) being situated above the most shallow points of the bed, and sin-type waves, when the maxima and the minima are located above the deepest points of the bed. Most importantly, the frequency ω_+ of the cos-type waves is larger than the frequency ω_- of the sin-type waves. These frequencies depend almost linearly on a squared (dimensionless) wave amplitude A_0, and the corresponding nonlinear shifts have been found both negative for bottom profiles used in the simulations (for example, see Figs. 1 and 2). In this situation, the cos-type waves are subjected to a modulational instability, which in the low-amplitude limit $A_0 \ll 1$ can be approximately described by a nonlinear Schrödinger equation with focusing nonlinearity; for $A_0 \sim 1$, there is no simplified model at the moment. The instability can sometimes become saturated with Bragg solitons or with similar structures. Indeed, after some time of evolution, formation of specific large-amplitude localized wave pulses has been observed in such systems. The pulses consist of a few nearly standing steep waves, which have peak-to-trough amplitude $h>0.4\Lambda$ (see Fig. 2). Though, unlike the analytical solutions for perfect Bragg solitons from the nonlinear optics (see Refs. [15–21]), these numerical localized water waves are not strictly time periodic, and we still may call them "Bragg quasisolitons," since their existence is caused by the same reasons, namely by the gap in the frequency spectrum and by the nonlinear frequency shifts. These water-wave Bragg quasisolitons are definitely interesting from a theoretical viewpoint, and they also seem potentially useful for practical applications.

Parameters of the numerical experiments. Exact explicit equations of motion exploited here have been derived in Ref. [26] from a variational formulation of the water-wave dynamics. A more simple way to obtain the same exact equations for two-dimensional ideal free-surface flows over an arbitrary topography, with possible extensions to time-dependent bottom profiles and to waves with constant vorticity, is described in Refs. [27,28]. In this paper we consider purely potential flows of an incompressible inviscid fluid over a static bottom. We take into account the gravity acceleration g and neglect surface tension. It is convenient to work with dimensionless variables as described below. Let us assume that the dimensionless gravity acceleration is $\tilde{g}=1$, and that a 2π-periodic bed has $K_0=200$ undulations. The dimensionless time $\tilde{t}$ is then related to the physical time $t=\tau\tilde{t}$ by a factor $\tau=(K_0\Lambda/2\pi g)^{1/2}$. For instance, the period of linear deep-water waves with the length $\lambda=2\Lambda$ is $T_*=(2\pi/\sqrt{100})\tau\approx 0.628\tau$, and their frequency is $\omega_*=2\pi/T_*$. The frequencies ω_+ and ω_- in Fig. 1 are shown normalized to ω_*.

We use a fixed analytic function $Z(\zeta)=x+iy$ of a complex variable $\zeta=\zeta_1+i\zeta_2$ to parametrize a bottom profile in the following way:

*ruban@itp.ac.ru

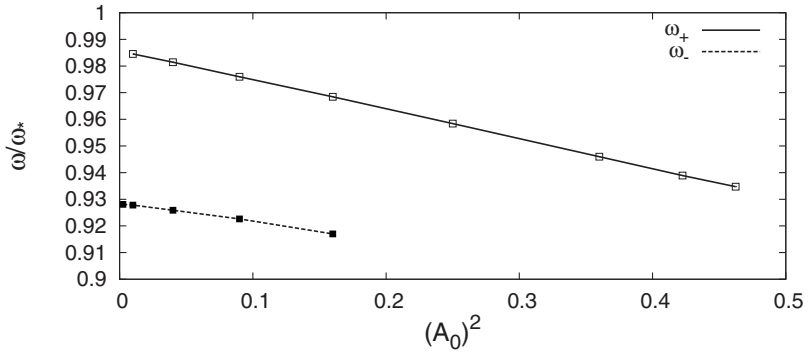

FIG. 1. Computed nonlinear frequency shifts for the two kinds of standing water waves over a nonuniform bed with the parameters $D_0=0.12$, $b=0.04$, $\epsilon=0$ (see text for details).

$$X^{(b)}(\zeta_1)+iY^{(b)}(\zeta_1)=Z(\zeta_1+i0). \tag{1}$$

In the numerical experiments described here, we chose $Z(\zeta)=\mathcal{B}(\zeta-i\alpha_0)$, where $\alpha_0=\pi/K_0$, and an analytic function $\mathcal{B}(q)$ is given by the formula

$$\mathcal{B}(q)=q-\frac{D_0}{K_0}(1+\epsilon\cos q)\frac{\sin(K_0q)}{[1+b\cos(K_0q)]}. \tag{2}$$

We fixed the parameters $D_0=0.12$ and $b=0.04$, while for a small modulation parameter ϵ we used the following values: $\epsilon=0.00$, 0.01, 0.02, and 0.05. The above form of $\mathcal{B}(q)$ gives the bottom shape as it is shown in Figs. 2–4 for $\epsilon=0.01$ (for $\epsilon=0.00$ it looks much the same, a difference is almost invisible). It is clear that we deal with an intermediate case between deep-water and shallow-water waves. It should be noted that the horizontal line $\zeta_2=\alpha_0$ maps to the horizontal line $y=0$, and therefore, due to the symmetry principle, the curvilinear coordinate system $[x(\zeta_1,\zeta_2),y(\zeta_1,\zeta_2)]$ is certainly valid for $0\le\zeta_2\le2\alpha_0$; in any case it is good for a surface elevation $|y|\lessapprox0.35\Lambda$, as it is seen from Figs. 2 and 5.

The profile of the free surface is parametrized by the formulas

$$X^{(s)}(\vartheta,t)+iY^{(s)}(\vartheta,t)=Z(\xi(\vartheta,t)), \tag{3}$$

$$\xi(\vartheta,t)=\vartheta+i\alpha(t)+[1+i\hat{R}_\alpha]\rho(\vartheta,t), \tag{4}$$

with unknown real functions $\alpha(t)$ and $\rho(\vartheta,t)$. The linear operator $\hat{R}_\alpha$ is diagonal in the discrete Fourier representation: in $[\hat{R}_\alpha\rho(\vartheta,t)]$ the mth Fourier harmonics

$$\rho_m(t)=\frac{1}{2\pi}\int_0^{2\pi}\rho(\vartheta,t)e^{-im\vartheta}d\vartheta$$

is multiplied by $R_\alpha(m)=i\tanh(\alpha m)$. We set initially $\alpha(0)=\alpha_0$ and $\rho(\vartheta,0)=0$, thus having the horizontal free surface $y=0$ at $t=0$.

The velocity field is determined through the surface value of the velocity potential $\psi(\vartheta,t)$. At $t=0$ we set $\psi(\vartheta,0)=A(\vartheta)(100)^{-3/2}\cos[100\vartheta+\gamma(\vartheta)]$. In the simplest case $A(\vartheta)=A_0=(0.15\ldots0.25)$, and $\gamma(\vartheta)=0$. Numerical results presented in Figs. 2–4 correspond to $A_0=0.2$.

The evolution of functions $\alpha(t)$, $\rho(\vartheta,t)$, and $\psi(\vartheta,t)$ is governed by explicit equations of motion (see [26–28]),

$$\dot{\alpha}(t)=-\frac{1}{2\pi}\int_0^{2\pi}\mathsf{Q}(\vartheta)d\vartheta, \tag{5}$$

$$\rho_t=-\mathrm{Re}[\xi_\vartheta(\hat{\mathsf{T}}_\alpha+i)\mathsf{Q}], \tag{6}$$

$$\psi_t=-\mathrm{Re}[\Phi_\vartheta(\hat{\mathsf{T}}_\alpha+i)\mathsf{Q}]-\frac{|\Phi_\vartheta|^2}{2|Z'(\xi)\xi_\vartheta|^2}-\tilde{g}\,\mathrm{Im}\,Z(\xi), \tag{7}$$

where $\Phi=(1+i\hat{\mathsf{R}}_\alpha)\psi$, and $\mathsf{Q}=(\hat{\mathsf{R}}_\alpha\psi_\vartheta)/|Z'(\xi)\xi_\vartheta|^2$. The linear operator T_α is diagonal in the discrete Fourier representation: $\mathsf{T}_\alpha(m)=-i\coth(\alpha m)$ for $m\neq0$, $\mathsf{T}_\alpha(0)=0$. All kinds of nonlinear interactions are taken into account in the above system of equations, unlike the situation in nonlinear optics, where approximate simplified equations for wave envelopes are used to derive analytic expressions for Bragg solitons (see, e.g., [15–21]). Equations (5)–(7) were simulated with a high accuracy (up to $N=2^{20}$ points in ϑ discretization), and results of the computations are discussed below.

Results and discussion. It was mentioned earlier that in the absence of the bottom modulation ($\epsilon=0$), the solution for $A(\vartheta)=A_0$ and $\gamma(\vartheta)=0$ is a purely standing nonlinear wave,

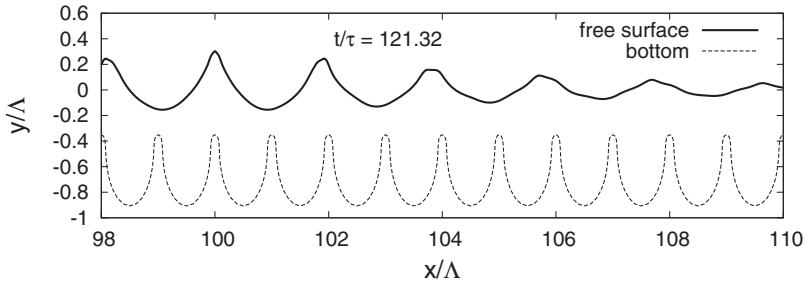

FIG. 2. Bragg quasisoliton at a moment when the surface elevation is high. The entire computational domain is $0\le x\le200\ \Lambda$, and the flow is symmetric about $x=100\ \Lambda$.

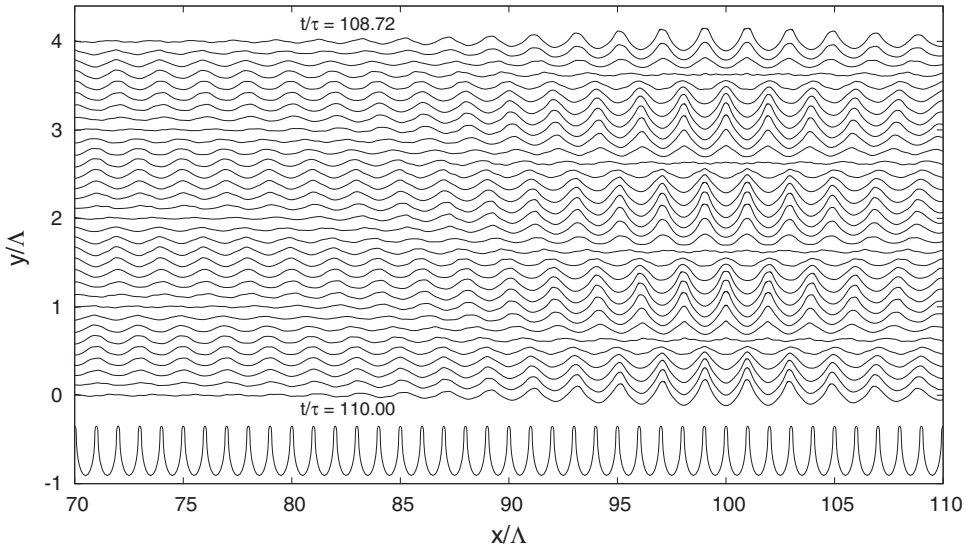

FIG. 3. Formation stage in evolution of a numerical water-wave Bragg quasisoliton. Here the free surface profiles are presented from $t/\tau=108.72$ to $t/\tau=110.00$ with the time interval $\Delta t/\tau=0.04$. The wave profiles, except the last one, are given vertically shifted for convenience. Also, the bed shape is shown, which is nearly periodic with a spatial period Λ (see text).

in the sense that the horizontal component of the velocity field is identically equal to zero at $x=l\Lambda$, for all integer l. However, the fluid motion inside each "cell" $l<x/\Lambda<(l+1)$ is periodic in time only approximately, and at $t>0$ the free surface is never strictly horizontal, so the potential energy never returns exactly to zero, just to a relatively small value (see, for example, Fig. 5). A nonzero ϵ and/or some nontrivial functions $A(\vartheta)$ or $\gamma(\vartheta)$ inevitably result in redistribution of the wave energy between "cells." In this dynamical process, participation is taken both by a coupling between the waves and the bottom, and by nonlinear interactions between the waves.

In a more general case $\epsilon\neq 0$, the dynamics of the free surface looks initially as a nearly standing wave, which however has a temporal phase $\phi^{(t)}\approx t\omega_+(\vartheta)$, with a weakly ϑ-dependent function $\omega_+(\vartheta)$. After some time, the gradient $\partial\phi^{(t)}/\partial\vartheta$ becomes sufficiently large, and then the second stage comes, when an amplitude modulation of the wave takes place. In this stage, there are some regions in the computational domain, where the wave is far from being purely standing (see Fig. 3). This second stage is ended with formation of a localized wave group consisting of a few high waves—a Bragg quasisoliton. A subsequent dynamics can be different depending on the initial parameters. For example, with relatively low initial amplitudes $A_0\leq 0.18$ and with $\epsilon=0.01$, we observed the quasisoliton to gradually decay after several dozens of wave periods (not shown). A different example is presented in Figs. 2–4, for $\epsilon=0.01$, $A_0=0.2$. In this case [and in many other cases which are not shown here, including nontrivial functions $A(\vartheta)$ and $\gamma(\vartheta)$ for $\epsilon=0$], the Bragg quasisoliton reaches such a high amplitude that wave crests in the maximum are nearly singular. In some simulations, double-peaked crests were observed. Thus, a kind of wave collapse can take place, which is, however, beyond our purely conservative model. Most probably, splashes will appear on the sharp crests in real situations.

Nonlinear processes in various physical systems, when they result in localization of the energy in the form of some coherent structures, are usually very important both for the fundamental theory and for practical applications. In particular, spatially periodic nonlinear media are known to support such highly energetic wave structures as Bragg solitons. In

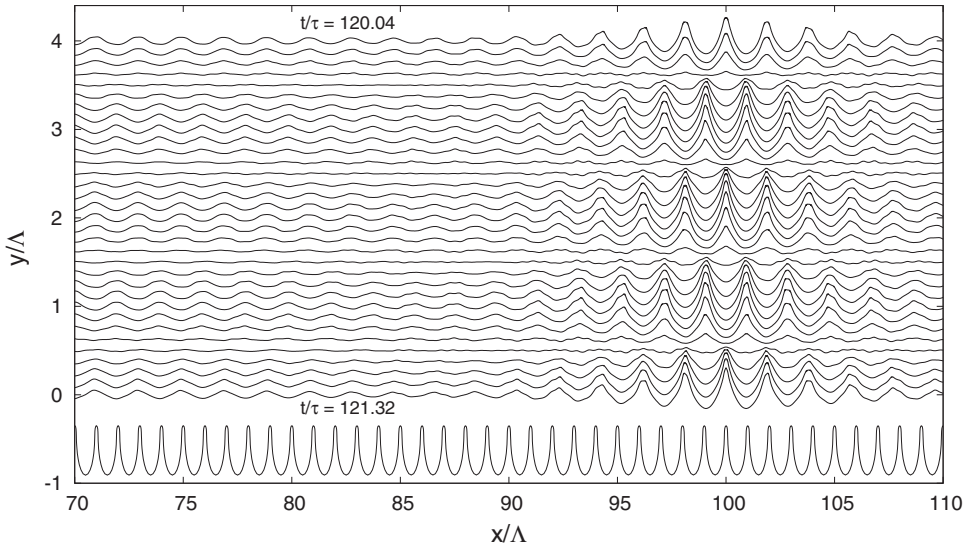

FIG. 4. Highly nonlinear stage in evolution of a water-wave Bragg quasisoliton. The free surface profiles are shown from $t/\tau=120.04$ to $t/\tau=121.32$ (compare to Figs. 2 and 3).

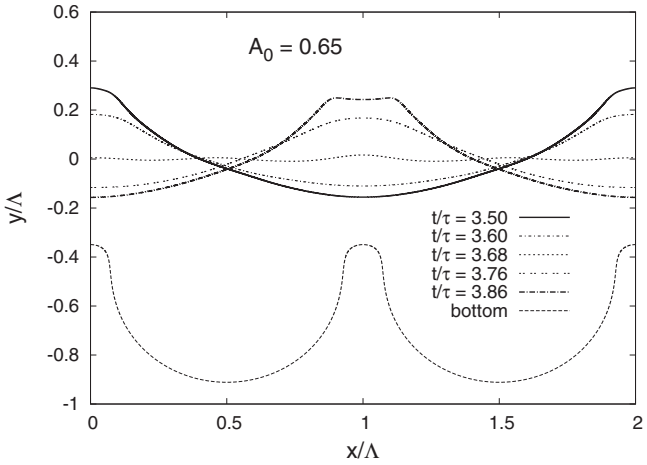

FIG. 5. A high-amplitude standing wave. Note the appearance of double-peaked crests.

the nonlinear optics, they have been studied for more than two decades. The present work predicts Bragg (quasi)solitons in the free-surface hydrodynamics. This prediction is based on accurate numerical solutions for finite-amplitude inviscid water waves in Bragg resonance with a strongly undulating nearly periodic bottom. Though in a real situation the bottom friction and other dissipative effects can sometimes modify the present results, the author believes water-wave Bragg quasisolitons will be observed experimentally, at least with $\Lambda \gtrsim 1$ m, when the dissipation is expected to be relatively weak. A length $L=50\ \Lambda$ of an experimental wave tank seems to be sufficient for that purpose.

These investigations were supported by RFBR Grant No. 06-01-00665, by RFBR-CNRS Grant No. 07-01-92165, by the "Leading Scientific Schools of Russia" Grant No. 4887.2008.2, and by the Program "Fundamental Problems of Nonlinear Dynamics" from the RAS Presidium.

[1] A. G. Davies and A. D. Heathershaw, J. Fluid Mech. **144**, 419 (1984).
[2] C. C. Mei, J. Fluid Mech. **152**, 315 (1985).
[3] T. Hara and C. C. Mei, J. Fluid Mech. **178**, 221 (1987).
[4] P. Devillard, F. Dunlop, and B. Souillard J. Fluid Mech. **186**, 521 (1988).
[5] M. Belzons, E. Guazzelli, and O. Parodi, J. Fluid Mech. **186**, 539 (1988).
[6] Y. Matsuno, J. Fluid Mech. **249**, 121 (1993).
[7] Y. Liu and D. K. P. Yue, J. Fluid Mech. **356**, 297 (1998).
[8] Y. Agnon, Phys. Rev. E **59**, R1319 (1999).
[9] Y. Agnon and E. Pelinovsky, J. Fluid Mech. **449**, 301 (2001).
[10] Zhen Ye, Phys. Rev. E **67**, 036623 (2003).
[11] H. B. Bingham and Y. Agnon, J. Fluid Mech. **24**, 255 (2005).
[12] J. T. Kirby, J. Fluid Mech. **162**, 171 (1986); Phys. Fluids A **1**, 1898 (1989); **5**, 380 (1993); http://chinacat.coastal.udel.edu/~kirby/
[13] W. Chen and D. L. Mills, Phys. Rev. Lett. **58**, 160 (1987).
[14] B. J. Eggleton, R. E. Slusher, C. M. deSterke, P. A. Krug, and J. E. Sipe, Phys. Rev. Lett. **76**, 1627 (1996).
[15] D. N. Christodoulides and R. I. Joseph, Phys. Rev. Lett. **62**, 1746 (1989).
[16] T. Peschel, U. Peschel, F. Lederer, and B. A. Malomed, Phys. Rev. E **55**, 4730 (1997).
[17] I. V. Barashenkov, D. E. Pelinovsky, and E. V. Zemlyanaya, Phys. Rev. Lett. **80**, 5117 (1998).
[18] A. De Rossi, C. Conti, and S. Trillo, Phys. Rev. Lett. **81**, 85 (1998).
[19] C. Conti, S. Trillo, and G. Assanto, Phys. Rev. Lett. **85**, 2502 (2000).
[20] T. Iizuka and C. Martijn de Sterke, Phys. Rev. E **61**, 4491 (2000).
[21] C. Conti and S. Trillo, Phys. Rev. E **64**, 036617 (2001).
[22] K. W. Chow *et al.*, Phys. Rev. E **77**, 026602 (2008).
[23] N. K. Efremidis and D. N. Christodoulides, Phys. Rev. A **67**, 063608 (2003).
[24] D. E. Pelinovsky, A. A. Sukhorukov, and Yu. S. Kivshar, Phys. Rev. E **70**, 036618 (2004).
[25] M. Matuszewski W. Krolikowski, M. Trippenbach, and Y. S. Kivshar, Phys. Rev. A **73**, 063621 (2006).
[26] V. P. Ruban, Phys. Rev. E **70**, 066302 (2004).
[27] V. P. Ruban, Phys. Lett. A **340**, 194 (2005).
[28] V. P. Ruban, Phys. Rev. E **77**, 037302 (2008).